https://doi.org/10.18321/cpc23(2)93-105

MРНТИ 29.03.31

Onset of thermal-diffusion instabilities in rich hydrogen/air premixed counter-flow twin flames

V. Bykov^{1*} and V. Gubernov²

¹Karlsruhe Institute of Technology (KIT), Institute of Technical Thermodynamics, Engelbert-Arnold-Strasse 4, Building 10.91 D-76131 Karlsruhe, Germany

²P.N. Lebedev Physical Institute of Russian Academy of Sciences, 53 Leninskiy Prospekt, 119991 Moscow, Russian Federation

ABSTRACT

The effect of flame instabilities onset in the counter-diffusion twin flame configuration is investigated numerically. The onset of instabilities in rich hydrogen/air combustion system is reported and properties of pulsating solutions are studied. Effects of mixture composition and strain rate as well as pressure are considered. Same as in the freely propagating rich hydrogen/air flames the onset of pulsations is promoted by pressure increase. The increased strain rate as expected stabilizes the flame for high values of the strain but found to promote the onset of instabilities for moderate values. Because the onset of oscillating flame behavior is extremely sensitive to molecular diffusion and chemical kinetics the outcome of the study can be directly checked in the experiments. The results of the parametric study near the boundary and the properties of both pulsating and steady solutions can be used for additional combustion models validation.

Keywords: counter-flow hydrogen flames, thermal-diffusion instabilities, pulsations onset, model validation.

1. Motivation and introduction

The onset of diffusive-thermal instabilities and flame pulsations are an interesting nonlinear dynamical phenomena by themselves, typically one observes this type of behavior shortly before the onset of flame extinction [1, 2]. This is because it is observed when the flame temperature is reduced due to heat losses, e.g. to the burner surface. As in a scenario with burner stabilized flames, which is reported in numerous asymptotic and numerical stability analyses performed in [3-14]. The other mechanisms is due to fuel dilution and decreasing of the adiabatic flame temperature. The onset of diffusive-thermal instabilities may result not only in extinction, but in generation of pulsating flames, reported and studied theoretically and numerically in a number of works [3, 10, 13] and are investigated and realized experimentally in [12, 14], were also determined and described in [15-18]. All these studies were performed for freely propagating

and burner stabilized flames. In these papers, the term diffusive-thermal pulsation instability was introduced and employed to denote this type of instability.

It has to be noted in freely propagating flames the onset of the pulsating diffusivethermal instability is also possible but only happen for large Lewis number, Le > 1. For instance, it cannot be observed in methane-air flames characterized by $Le \approx 1$. Though, as it has been shown analytically and numerically and demonstrated in [5, 10] within the thermal-diffusive models the heat losses to the surface of the burner enhances the onset of pulsating instabilities, which may occur even for Lewis number less or equal to one. In [19–22] the dynamical flame regimes having different and multi-dimensional oscillating behavior in space have been investigated and reported for both low and normal pressure conditions. These include pulsating axial, radial, drumhead modes, target and spiral waves.

The possibility to use these regimes as a tool for the verification of the detailed reaction mechanisms was proposed and investigated in a number of studies, for instance, this approach was successfully

*Ответственный автор E-mail: viatcheslav.bykov@kit.edu

Дата поступления: 10 мая 2025 г.

applied to methane-air [15–17] and methane-hydrogenair [18] flames at normal pressure. There experimentally measured and numerically calculated characteristics of the pulsating flame were compared and it was shown that quantitative comparison is possible keeping the flow close to 1D spacial structure.

The way to enrich the experimental data with controlled flow conditions in the transient combustion scenario is of primary importance because the validation of reaction mechanisms and reaction rate parameters' estimation is an example of an ill-posed mathematical problem. There is always a lack of available experimental data that can be used to estimate these parameters. The data with well controlled uncertainty delivering observables with high accuracy in sensitive scenario as pulsating flames and onset of oscillations are highly demanded. Then it might lead to posing and improving the situation with the inverse problem of finding reaction rate constants.

Because the rich mixtures exhibit instabilities it can be worthwhile to consider strained flames configuration as one of most important standard academic configurations to study both premixed and non-premixed flames as the counter-flow flame. There are a lot of studies available in the literature concerning experimental, analytical and numerical investigations of the effect of both stretch and curvature on the flame characteristics [23, 24]. The fact that in this configuration the one-dimensional formulation is possible makes it additionally important and counter-flow planar, spherical and cylindrical flames can be taken into account. This has already been demonstrated in [25, 26], where the tubular flame configuration is formulated by using only a single spatial dimension whing the Lagrangian coordinates. This can be used to simplify the numerical analysis considerably. In this way experimental data with tubular flames considered in [27-29] show that stretch rates comparable to those of a flat counter-flow configuration can be achieved. Though the case with spherical and cylindrical symmetries may be employed to single out and separate the stretch and curvature phenomena. In this study, however, the focus is made on the pure counter-flow planar configuration.

The combined effect of strain, composition and pressure on the onset of pulsating diffusive-thermal instabilities and flame structure in the oscillating regimes is investigated similar to [14, 30]. The counter-flow configuration is in the focus of this

pure computational study and follows the main steps of the case of a tubular flame configuration investigated in details in [31]. In order to set-up such an analysis a test case of rich mixtures near the stability boundary is considered and used for the twin flame configuration. The flame dynamics is studied under varying pressure, composition of the mixture on the one of opposed nozzles and strain rates. Characteristics and critical parameters for the onset of flame oscillations are determined and discussed for rich premixed hydrogen-air flames. The outline of the study is following. The mathematical model with main physical assumptions made to address the phenomenon. Then the numerical approach and computational procedure to integrate the system in the considered configuration is outlined. In the results section, three different parametric studies are described and discussed showing the characteristics of pulsating solutions, their emergence and and twin flame stabilization once the parameter fall below the critical values.

2. Mathematical model

The opposed axial-symmetric nozzle configuration is considered to be infinite along the direction of symmetry (z-axis vertical) in cylindrical coordinates (see Fig. 1). The mathematical model and numerical algorithm for solving the system of the governing equations employed in the current work are based on a formulation of the governing equation system described in [32].

A system of conservation equations with detailed chemical reaction mechanisms and detailed transport models is considered. Then the system of governing equations can be written as

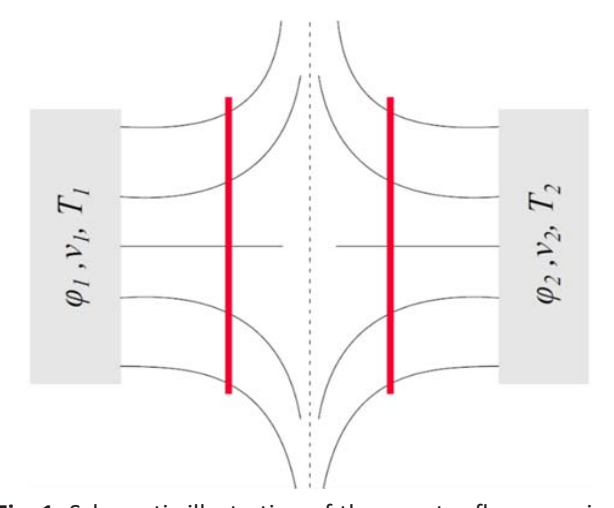


Fig. 1. Schematic illustration of the counter flow premixed twin flame configuration.

$$\frac{\partial \rho}{\partial t} + 2\rho G(r) + \frac{\partial (\rho \nu_r)}{\partial \nu_r} = 0 \tag{1}$$

$$\frac{\partial G(r)}{\partial t} + \frac{1}{\rho}J + G(r)^{2} - \frac{1}{\rho}\frac{\partial}{\partial r}\left(\mu\frac{\partial G(r)}{\partial r}\right) + \upsilon r\frac{\partial G(r)}{\partial r} = 0$$
 (2)

$$\frac{\partial v_r}{\partial t} + \frac{1}{\rho} \frac{\partial P}{\partial r} + \frac{4}{3\rho} \frac{\partial}{\partial r} \left(\mu G(r) - \mu \frac{\partial v_r}{\partial r} \right) - \frac{2\mu}{\rho} \frac{\partial G(r)}{\partial r} + v_r \frac{\partial v_r}{\partial r} = 0 \quad (3)$$

$$\frac{\partial \omega_{i}}{\partial t} = \frac{\dot{\omega}_{i} M_{i}}{\rho} - \upsilon_{r} \frac{\partial \omega_{i}}{\partial r} + \frac{1}{\rho} \frac{\partial}{\partial r} \left(\rho D_{i}^{D} \frac{\omega_{i}}{x_{i}} \frac{\partial x_{i}}{\partial r} + \frac{D_{i}^{T}}{T} \frac{\partial T}{\partial r} \right)$$
(4)

$$\frac{\partial T}{\partial t} = \frac{1}{\rho C_p} \sum_{i=1}^{n_s} \left(\dot{\omega}_i h_i M_i + c_{pi} \left(j_{i,r} \frac{\partial T}{\partial r} \right) \right) + \frac{1}{\rho C_p} \frac{\partial}{\partial r} \left(\lambda \frac{\partial T}{\partial r} \right) - \upsilon_r \frac{\partial T}{\partial r}$$
(5)

The detailed molecular transport is based on the Curtiss-Hirschfelder approximation [33, 34] for mixture averaged diffusion coefficients D_i^D in Eq. (4) including thermal diffusion (Soret effect - D_i^T) (see e.g. [35]) thus defining the mass flux density in Eqs. (1) and (5) by

$$j_{i,r} = \rho D_i^D \frac{\omega_i}{x_i} \frac{\partial x_i}{\partial r} + \frac{D_i^T}{T} \frac{\partial T}{\partial r}$$
 (6)

In the equations above t and r are the time and distance in cylindrical coordinates, T is the temperature, w_i is the mass fraction and x_i the mole fraction of species i; ρ , cp, and λ are the density, the constant pressure specific heat capacity, and the heat conductivity of the mixture, respectively; $c_{\rho i}$, M_i , ω_i , h_i , and j_i are the constant pressure specific heat capacity, the molar mass, the chemical rate of production, the specific enthalpy, and the diffusion flux density of species i. \overline{M} is the mean molar mass, D_i^D the diffusion coefficient for species i, and D_i^T is the thermal diffusion coefficient.

2.1. Physical assumptions

Starting with the governing equations for a twodimensional axial symmetry configuration and using the assumptions in [32], namely,

- species mass fractions and temperature w_i , T are functions only of the coordinate normal to the flame, i.e. in r-direction;
- v_r normal to the flame velocity is only a function of r;
- -tangential velocity gradient is $v_z = z \; G(r)$ providing with $G(r) = \frac{\partial v_z}{\partial_z}$ the only function of r;

- the solutions considered on the symmetry axes r, where z = 0. Note here unusual coordinates notation are used along the symmetry axes r and z in radial direction of the diverging flow of products (r, z);
- constant pressure due to low Mach number approximation;
- the axial / tangential pressure gradient is assumed to obey $(1/z)\partial p/\partial z = J = const.$ (see [32]);
 - the ideal gas law $P = \rho RT/\overline{M}$ is valid.

Under the assumptions made there is no need to solve for the radial velocity component, because *J* is constant and the assumption close the system of equations Eq. (1-6). Now, only boundary conditions need to be specified to enable the numerical integration of the system.

2.2. Boundary and initial conditions

The burner nozzles have a large thermal inertia and thickness. Thus, it is assumed that the porous medium of the burner surfaces remain at constant temperature T_o , i.e. the burner surface might be thermally stabilized in the experiments to yield the boundary conditions below when the nozzles are getting close one to the other.

$$T = T_{o}, \quad w_{i} = w_{i,l} \quad \rho \ v = (\rho v)_{l} \ r = R_{b}$$

 $T = T_{o}, \quad w_{i} = w_{i,r} \quad \rho \ v = (\rho v)_{r} \ r = R_{r}$ (8)

where $w_i^{l,r}$ denotes the mass fraction of species i on the left and right nozzles at $r=R_{l,r}$ positions in the space, which is fed into the burner and $\rho_{l,n}v_{l,r}$ is the density and velocity of inflowing mixtures at the nozzle. The surface of the burner is cold ($T_0=298$ K) and flames considered are typically far away from the burner surface. Remark that because the quantity of tangential pressure gradient $J=(1/z)\partial P/\partial z$ that defines the strain of the flow is constant $-a=(-J/\rho)^{1/2}$ 1/s, one can specify the strain rate and only one boundary condition for velocity, say on the left side such that the stagnation point remains in the center of computational domain, and thus the other inflow conditions on the right hand side will be defined automatically.

In the study the Warnatz's mechanism [32, 35], which includes 38 elementary reactions taking place between nine species (H_2 , H, H_2O , H_2O_2 , OH_2 , N_2 , O, O_2 , OH) is used. Note that this mechanism is considered as a representative example only and the outcome of the study should not be qualitatively affected by the usage of a particular mechanism. Though as it is shown below the phenomenon is very

sensitive to system parameters and models used, which is actually the reason to consider and use the onset and pulsating characteristics for additional combustion model validation. It is demonstrated that both the onset of pulsating regimes and their characteristics are very sensitive to the chemical and diffusion properties of the mixture.

3. Numerical method

The numerical treatment of the 1D configuration is based on method of lines [35]. Spatial discretizations of the partial differential equation system, which is defined on a non-equidistant grid using finite differences (central differences for the transport terms and upwind differences for the convective terms) results in a large differential / algebraic equation system, which is solved by the linearly implicit extrapolation method LIMEX [36, 37] with error, order, and step size control. The spatial grid is statically adapted based on the magnitude of the local gradients and curvature of the dependent variables (see [35] for details). This altogether allows to integrate the system very accurately both in time and in space, which is very crucial for transient flame propagation regimes considered in the study.

In the numerical integration the temperature of the inflow gas is in all cases T_0 = 298 K, while pressure - P, mass flux of the fresh mixture at nozzles kept constant with both inflow mass flux density - ρv and the equivalence ratio - ϕ are varied in the parametric study. The governing system of equations Eqs. (1-5) is integrated numerically for the given parameters until the solution converges either to a steady combustion front or to a periodically pulsating solution. In the latter case, the time integration is stopped, once the periodic solution is found, i.e. when the amplitude of oscillations is not changing and e.g. $x_i(x,t) = x_i(x,t+\tau)$ is satisfied, where τ defines a period of flame oscillations and x_i is species mole fraction.

The initial solution profile is taken in the parameter space - (P, v, ϕ) . The loss of stability of the steady combustion fronts is analyzed numerically similar as described in [14, 30, 38].

4. Results and discussion

In the parameter space the control parameters $(P, v \text{ and } \phi)$ are fixed except for one, which will be varied near the onset of instabilities and formation of the periodically oscillating flames. Typically, the

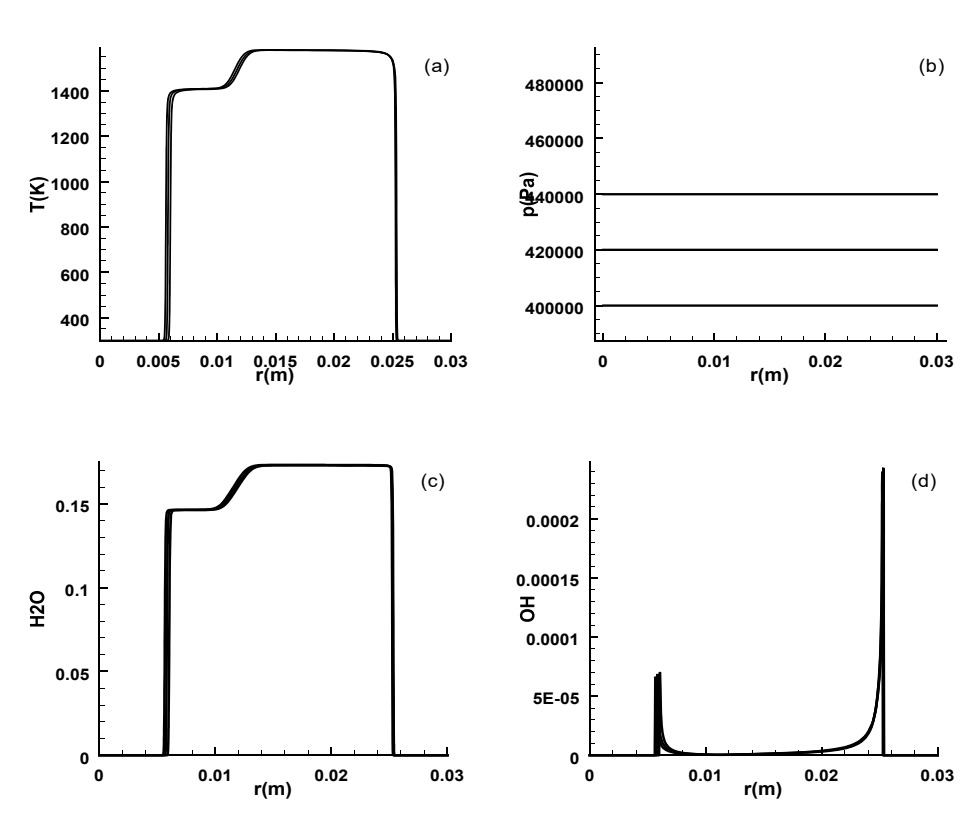


Fig. 2. The structure of the twin flame for $\phi = 5$, $\phi = 4$ and P = 4.0,4.2,4.4 bar. Solid lines - steady solution profiles of species mole fractions for the inflow mass flux density - $\rho v = 2.5 \text{ kg/m}^2\text{s}$.

solutions are integrated from the case of steady flame and the parameter of interest is gradually increased/decreased until flame pulsations emerge. The amplitude of the oscillations is traced by choosing an observable variable, e.g. temperature or x_{OH} mole fractions etc., to monitor the time history and distinguish periodic behavior. The local maximum of x_{OH} distribution can be an example of such observable. The neutral stability boundary, when the pulsations onset, in the space of parameters can be identified by repeating this procedure for different values of a control parameter.

4.1. Pressure variation

The numerical analysis of freely propagating flame, i.e. no strain, preformed in [39, 40] reveals that the phenomenon is extremely sensitive to the combustion models used to describe the onset. Moreover, the critical value for the onset of pulsation for rich hydrogen / air flame for $\phi = 5$ was estimated to be about P = 5 bar (see [39], Fig. 2). Accordingly the following set-up is suggested to be used to study the strained premixed flame near the stability boundary, namely, $\phi = 5$ on the left boundary, while keeping the lower value for stoichiometry on the

right - ϕ = 4, keep the strain constant at moderate values ρv = 2.5kg/m²s such that the flame fronts remain relatively far away from the boundary but still separated from each other. Then the pressure is varied from P = 4 to P = 5 bar in steps of 0.2 bar.

Fig. 2 shows the temperature, pressure, H₂O and OH mole fractions profiles of the steady twin flame fronts. One can see the pressure remains constant along the computational domain, while temperature, vapor distribution shows similar behavior and demonstrates strong gradient within the flame front standing at a distance to each other as well as to the boundaries. A local maximum of OH radicals is observed at these locations. The differences in maxima and in asymmetric profile are due to various compositions provided at the right and left boundaries. Because the pressure variation is not that significant all the profiles are close to one another and look very similar.

In the Fig. 3 in contrast to Fig. 2 for pressure P > 4.6, which is close to the critical one, the steady solution ceases to exist and oscillations emerge. The twin flame profile slightly shifts in space reflecting the pulsating solution shown in Fig. 3(a) by different color - black, blue and cyan for P = 4.6, 4.8, 5.0 bar correspondingly. The local maximum of OH shifts

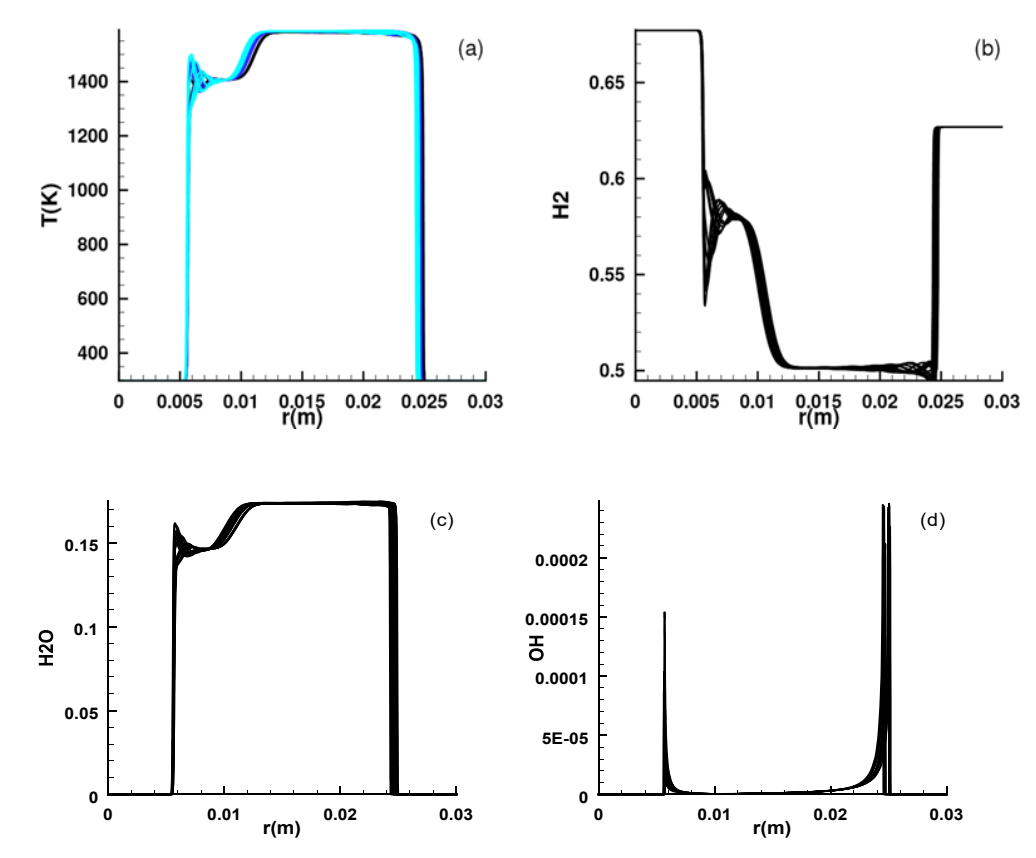


Fig. 3. The structure of the twin pulsating flame for ϕ = 5, ϕ = 4 and P = 4.6,4.8,5.0 bar. Solid lines pulsating solution profiles for some instances of time along the period of oscillations of species mole fractions for the inflow mass flux density - ρv = 2.5 kg/m²s.

and oscillates also in the amplitude showing the influence of the pulsations onto the flame structure. This can also be seen in, e.g. Fig. 3(b), where instead of pressure H_2 mole fraction profiles for pulsating solutions are shown. One can observe increasing amplitudes of both oscillations in space and for amplitudes of profiles once the pressure increases similarly as in the freely propagating flame.

It is interesting that the critical values for pressure at the onset of oscillations shift towards lower values of the pressure $P^* = -4.5$ instead of $P^* =$ 5.2 shown for freely propagating flame. This is not strange and can be explained by the effect of the strain that generally pushes the systems state on the solution profile further away from the equilibrium. Thus, the system solution gets more vulnerable to perturbations leading the lower pressures although the interactions between the flames are there, it does not succeed to stabilize the flame. The strain yet is not strong enough. The pure effect of the strain is addressed in the next subsection. The purpose is to find out parameter range to separate the profiles in space near the critical value, study and show the effect of the strained flow onto the structure of the twin flame.

4.2. Strain variation

In order to see distinguished profiles near the stability limit the mixture composition is taken constant ϕ = 5 on the left and ϕ = 4 on the right for pressure exceeding the stability limit P = 5.5 > P^* = 4.6 with moderate strain rate defined by the inflow mass flux density - ρv = 2.5 kg/m²s shown in Fig. 3, then the strain rate is varied. The inflow mass flux density first increased to ρv = 14.0 kg/m²s, then three different values are taken to reduce the strain rate, accordingly ρv = 10.0, 8.0, 4.0 kg/m²s, to find out how the reduced strain influences the onset and properties of oscillations.

It turns out the critical value is attained between $\rho v = 10.0 \text{ kg/m}^2 \text{s}$ and $\rho v = 8.0 \text{ kg/m}^2 \text{s}$ and the flames start oscillating with the increase of amplitudes towards smaller values of ρv . As far as a critical condition is met the flame becomes unstable and oscillations emerge near the richer side while the structure of the leaner part of the twin flame remains almost unperturbed for relatively high strain rate and only oscillates in the space due to onset of pulsating solutions on the left/richer side. There the oscillations become pronounced and observed for almost all dependent systems state variables (see Figs. 4(a)-(d)).

The steady flame fronts for two inflow rates show differences for OH radical on the richer and leaner sides. Fig. 4(d) shows the maxima on the rich side is observed but almost vanities on the richer side (on the left), while for leaner side $\phi = 4$ max of OH can be seen and becomes slightly increased when the oscillations onset. The other Figs. 4(a)-(c) clearly show by differences between magenta and blue lines that with the decrease of the strain the amplitudes of the pulsations on the leaner case with respect to the position of the flame front (see the max of gradients on the left). It signifies that the onset is triggered on the richer side and the populations are propagate and influence the flame structure on the leaner side and the balance within the flame front of the right flame is slightly perturbed such that the flame front shifts in space in attempt to find out stable position given the oscillating velocity field due to onset of oscillations coming form the left.

Because the gas mixture composition on both sides remains the same the structure for the reduced strain rates (blue and magenta lines on Figs. 4(a)-(d)) remains very similar both for educt and products except spacial distribution and flame front amplitudes in space. In order to study and to show how the composition is changing the system solution properties in both steady and pulsating regimes the flow conditions and pressure is fixed next while mixture composition is varied the following subsection.

4.3. Mixture composition variation

Now, pressure is fixed to P=5.0 bar, which is also beyond the critical value for moderate strain rate attained with $\rho v=7.5$ kg/m²s, that is kept fixed as well, while the mixture composition on the right boundary is varied with $\phi=4.0, 4.5, 5.0$, correspondingly.

Fig. 5 show the three typical solution profiles near the stability limit. As before the black lines correspond to the steady solution profiles for lower/leaner mixtures before the oscillations onset - ϕ = 4.0, 4.5. The case of ϕ = 4.0 is evident since in this case the twin flames are symmetric (see Fig. 5(a) for temperature) because the same composition is streaming from both sides. Then the composition becomes richer and the temperature of the first (on the left) flame is reduced the flow conditions are kept the same. The mixture becomes less reacting in this case and hence the flames move closer together that can be seen in the reduced distance between the flame fronts. At the same time the symmetry

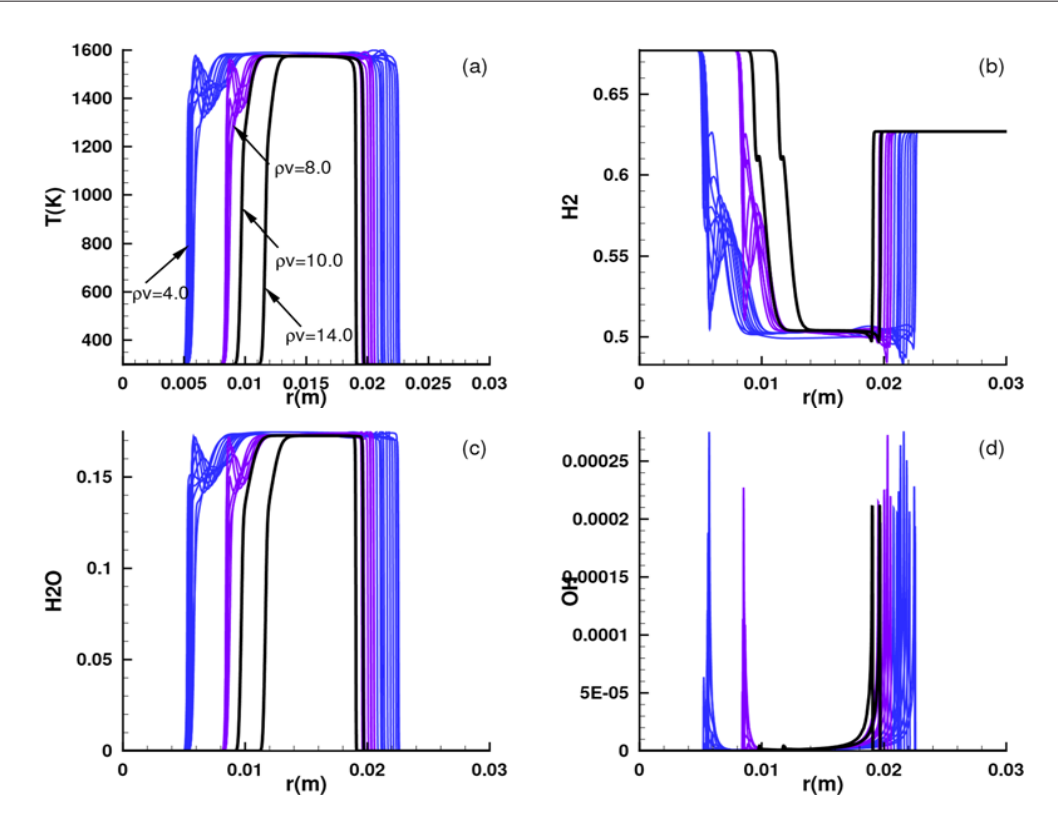


Fig. 4. The structure of the twin steady and pulsating flame for $\phi = 5$, $\phi = 4$ and P = 5.5 bar. Solid black lines are steady solution profiles for $\rho v = 14.0,10.0$ kg/m²s while magenta and blues lines signify pulsating solution profiles of species mole fractions for some instances of time along the period of oscillations for the inflow mass flux density - $\rho v = 8.0,4.0$ kg/m²s.

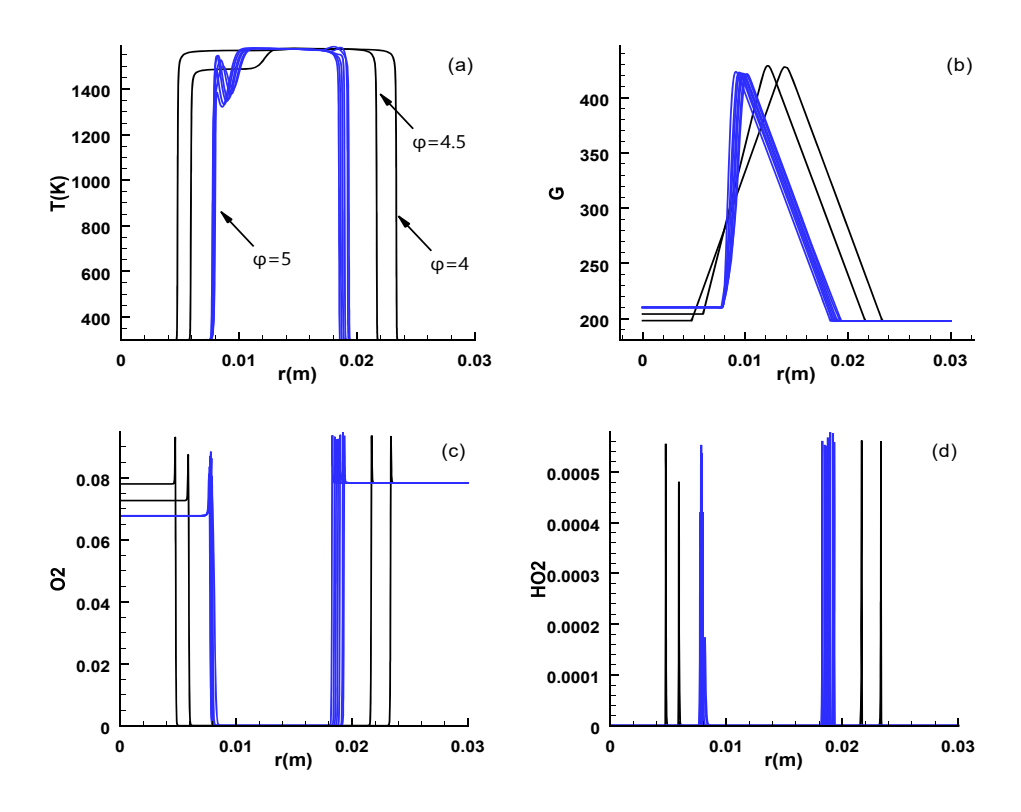


Fig. 5. The structure of the twin pulsating flame for ϕ = 4.0, 4.5, 5.0 on the left boundary, while ϕ = 4.0 fixed on the right for P = 5.0 bar. Solid black lines - steady solution profiles for ϕ = 4.0, 4.5 cases and blue lines are pulsating solution (for ϕ = 5.0) profiles of species mole fractions at some instances in time along the period of oscillations for the constant inflow mass flux density - ρv = 7.5 kg/m²s.

is lost, shown by Fig. 5(b), where the tangential velocity gradient ($G = \partial_{vr}/\partial_r$) starting from being perfectly symmetric changes the form, such that the gradients towards reacher side steadily increase.

Once the oscillations onset shown by blue profiles in Figs. 5 a typical pattern of pulsating behavior is observed similarly as before with both hanging flame structure on the left and shifting the relatively stable flame front for leaner mixture on the right. This can be seen by looking at the HO₂ radical profiles shown on Fig. 5(d), which illustrates slight reduction in the maximum value for $\phi = 4.5$ and then when pulsations emerge (re-emerge again at ϕ = 5) the maximum over the period reaches almost the same value as attained for the case of ϕ = 4.0. The maximum of HO₂ mole fraction presented on the right figure illustrates additionally periodic character of the pulsating regime. The loss of symmetry as well as oscillation on space of the leaner side flame front can also be seen on Fig. 5(c) shown for another main reactant - O₂ of the combustion systems considered.

4.4. Summary and outlook

Three cases of computational studies of independent parameter variation for the onset and pulsating solutions in the premixed counterflow formulation show very similar behavior near the neutral stability boundary. Table 1 summarizes the parameters for all three cases. The parameters are chosen to be close to those observed in the freely propagating flame of the hydrogen air rich combustion systems. Remark that the tangential pressure gradients J are provided to ensure the flames are positioned in the center of the computational domain. It is kept constant for pressure and composition variations (Cases I and III), but when the inflow condition on the left side is changed (Case II) it has to be corrected / tuned to ensure the balance of the inflow conditions and keep position of the flames in the middle.

In the considered range of the equivalence ratio depending on the pressure and strain rate one of the twin flames losses the stability and oscillating flame front behavior is emerged. Same as freely propagating flame pressure increase promotes the onset as well as the mixture composition. The strain however first stabilizes the flame, but being reduced might even promote the onset of pulsations if compared to the freely propagating flames. This is important for experimental observations since the freely propagating flames are difficult to arrange in the experiments, while counter-flow configuration can be arranged and studied much easily. The study is an evidence that such experiments can also be used to trace the onset of instabilities and to use these experiments to additionally verify combustion models. Hence when both experiments can be performed with well controlled conditions to make sure close to 1D flame behavior and computations can be carried out to yield and to reproduce the transient solution properly. The results obtained can be considered as a proof of the concept and the only first step to achieve the goal of extending the data for reliable validation. This might be crucial for validation of combustion model to describe the flame behavior near the extinction and flammability limits. The latter can be extremely important to develop efficient combustion facilities with well controlled combustion processes.

5. Conclusions

The very rich hydrogen-air premixed counterflow twin flames are considered in the study for just a limited set of systems parameters, namely, different inflow conditions, ambient pressures and equivalence ratio. The parameters were chosen to be close to those of freely propagating flame near the onset of thermal-diffusion instabilities.

Table 1. Parameters of three cases considered; Cases I-III are pressure, mass flux density and mixture composition variations. The only constant conditions are equivalence ratio on the right boundary - ϕ = 4.

Case I							
Р	φ	ρν	J				
4.0	5.0	2.25	-4.5×10^{-4}				
4.2	5.0	2.25	-4.5×10^{-4}				
4.4	5.0	2.25	-4.5×10^{-4}				
4.6	5.0	2.25	-4.5×10^{-4}				
4.8	5.0	2.25	-4.5×10^{-4}				
5.0	5.0	2.25	-4.5×10^{-4}				

	Case II				
ρν	Ρ	φ	J		
14.0	5.5	5.0	-1.5×10^{-5}		
10.0	5.5	5.0	-1.5×10^{-5}		
8.0	5.5	5.0	-1.5×10^{-5}		
4.0	5.5	5.0	-1.5×10^{-5}		

Case III						
φ	Ρ	ρν	J			
4.0	5.0	7.5	-9.5×10^{-4}			
4.5	5.0	7.5	-9.5×10^{-4}			
5.0	5.0	7.5	-9.5×10^{-4}			

The onset of pulsations was investigated when in the parameter space either pressure, strain or composition reaches a critical value. This indeed was observed to be close to the one for freely propagation - ϕ = 5.0, P^* = 5.2 bar. It was shown that the pressure and richer compositions promote the onset of instantiates as in freely propagating flames. At the same time it was demo started that the moderate strain in a combination with leaner mixture of the second twin flame has also promoted the onset of pulsations with critical pressure reduction to P^* = 4.6 bar. However, in the case the strain was increased the flame stabilizes and the instabilities get suppressed by the inflow conditions.

The study has shown that the suggested configuration can be used to elaborate interplay between strain, pressure and mixture composition to ensure well controllable and well observable onset of oscillation and pulsation characteristics of the flames. It can be used as an additional generic set-up, which is very interesting and promising to further verify detailed chemical kinetics and diffusion models for hydrogen combustion processes in transient regimes.

6. Acknowledgments

This project received partial financial support from the German Research Foundation (DFG) within the projects SFB/TRR 150 (project number 237267381).

Список литературы (ГОСТ)

- [1]. Gubernov V., Kolobov A., Polezhaev A., Sidhu H., Mercer G. Period doubling and chaotic transient in a model of chain-branching combustion wave propagation // Proc. R. Soc. A. 2010. Vol. 466, № 2121. P. 2747–2769.
- [2]. Kurdyumov V.N., Gubernov V.V. Dynamics of combustion waves in narrow samples of solid energetic material: Impact of radiative heat losses on chaotic behavior and dynamical extinction phenomenon // Combust. Flame. 2020. Vol. 219. P. 349–358.
- [3]. Margolis S.B. Bifurcation phenomena in burnerstabilized premixed flames // Combust. Sci. Technol. – 1980. – Vol. 22, № 3–4. – P. 143–169.
- [4]. Matkowsky B.J., Olagunju D.O. Pulsations in a burner-stabilized premixed plane flame // SIAM J. Appl. Math. – 1981. – Vol. 40, № 3. – P. 551–562.
- [5]. Buckmaster J. Stability of the porous plug burner

- flame // SIAM J. Appl. Math. 1983. Vol. 43, № 6. P. 1335–1349.
- Joulin G. Flame oscillations induced by conductive losses to a flat burner // Combust. Flame. 1982.
 Vol. 46. P. 271–281.
- [7]. McIntosh A. On the cellular instability of flames near porous-plug burners // J. Fluid Mech. – 1985.
 – Vol. 161. – P. 43–75.
- [8]. Kaper H.G., Leaf G.K., Matkowsky B. On the stability of the porous plug burner flame // Combust. Sci. Technol. – 1986. – Vol. 47. – P. 93–101.
- [9]. Chao B.H., Law C.K. Duality, pulsating instability, and product dissociation in burner-stabilized flames // Combust. Sci. Technol. – 1988. – Vol. 62, № 4–6. – P. 211–237.
- [10]. Kurdyumov V.N., Matalon M. The porous-plug burner: Flame stabilization, onset of oscillation, and restabilization // Combust. Flame. 2008. Vol. 153, № 1. P. 105–118.
- [11]. Chao B.H. Instability of burner-stabilized flames with volumetric heat loss // Combust. Flame. 2001. Vol. 126, № 1. P. 1476–1488.
- [12]. Kurdyumov V.N., Sánchez-Sanz M. Influence of radiation losses on the stability of premixed flames on a porous-plug burner // Proc. Combust. Inst. 2013. Vol. 34, № 1. P. 989–996.
- [13]. Margolis S.B. Effects of selective diffusion on the stability of burner-stabilized premixed flames // Symp. (Int.) Combust. 1981. Vol. 18. P. 679–693.
- [14]. Gubernov V., Bykov V., Maas U. Hydrogen/air burner-stabilized flames at elevated pressures // Combust. Flame. 2017. Vol. 185. P. 44–52.
- [15]. Nechipurenko S., Miroshnichenko T., Pestovskii N., Tskhai S., Kichatov B., Gubernov V., Bykov V., Maas U. Experimental observation of diffusivethermal oscillations of burner stabilized methaneair flames // Combust. Flame. – 2020. – Vol. 213. – P. 202–210.
- [16]. Mislavskii V., Pestovskii N., Tskhai S., Kichatov B., Gubernov V., Bykov V., Maas U. Diffusive-thermal pulsations of burner stabilized methane-air flames // Combust. Flame. 2021. Vol. 234. P. 111638.
- [17]. Moroshkina A., Mislavskii V., Kichatov B., Gubernov V., Bykov V., Maas U. Burner stabilized flames: Towards reliable experiments and modelling of transient combustion // Fuel. – 2023. – Vol. 332. – P. 125754.
- [18]. Moroshkina A., Yakupov E., Mislavskii V., Sereshchenko E., Polezhaev A., Minaev S., Gubernov V., Bykov V. The performance of reaction mechanism in prediction of the characteristics

- of the diffusive-thermal oscillatory instability of methane-hydrogen-air burner-stabilized flames // Acta Astronaut. 2024. Vol. 215. P. 496–504.
- [19]. Mapp J.W., Blackshear J.I., Gorman M. Short communication // Combust. Sci. Technol. – 1985. – Vol. 43. – P. 217–225.
- [20]. El-Hamdi M., Gorman M., Mapp J.W., Blackshear J.I. Stability boundaries of periodic models of propagation in burner-stabilized methane-air flames // Combust. Sci. Technol. 1987. Vol. 55. P. 33–40.
- [21]. Pearlman H. Target and spiral wave patterns in premixed gas combustion // J. Chem. Soc. Faraday Trans. 1997. Vol. 93. P. 2487–2490.
- [22]. K. Robbins, M. Gorman, J. Bowers, R. Brockman Spiral dynamics of pulsating methane-oxygen flames on a circular burner // Chaos. 2004. Vol. 14. P. 467–476.
- [23]. Law C.K. Combustion Physics. Cambridge: Cambridge Univ. Press, 2010. 771 p.
- [24]. Warnatz J., Maas U., Dibble R.W. Combustion. Berlin: Springer, 2006. 387 p.
- [25]. Dixon-Lewis G. Structure of laminar flames // Symp. (Int.) Combust. 1991. Vol. 23. P. 305–324.
- [26]. Smooke M. Numerical modeling of the structure and properties of tubular strained laminar premixed flames // Dyn. Deflagr. React. Syst. 1991. Vol. 131. P. 125.
- [27]. Ishizuka S. An experimental study on extinction and stability of tubular flames // Combust. Flame. 1989. Vol. 75. P. 367–379.
- [28]. Kobayashi H., Kitano M. Extinction characteristics of a stretched cylindrical premixed flame // Combust. Flame. – 1989. – Vol. 76. – P. 285–295.
- [29]. Ogawa Y., Saito N., Liao C. Burner diameter and flammability limit measured by tubular flame burner // Symp. (Int.) Combust. 1998. Vol. 27. P. 3221–3227.
- [30]. Korsakova A., Gubernov V., Kolobov A., Bykov V., Maas U. Stability of rich laminar hydrogenair flames in a model with detailed transport and kinetic mechanisms // Combust. Flame. 2016. Vol. 163. P. 478–486.
- [31]. Bykov V., Gubernov V., Maas U. Combustion of near stoichiometric hydrogen-air mixtures stabilized near tubular porous burner // Combust. Plasmochem. 2022. Vol. 20. P. 277–278.
- [32]. Stahl G., Warnatz J. Numerical investigation of time-dependent properties and extinction of strained methane and propane-air flamelets // Combust. Flame. 1991. Vol. 85. P. 285–299.

- [33]. Giovangigli V. Mass conservation and singular multicomponent diffusion algorithms // IMPACT Comput. Sci. Eng. 1990. Vol. 2. P. 73–97.
- [34]. Ern A., Giovangigli V. Multicomponent Transport Algorithms. Berlin: Springer, 1994. 398 p.
- [35]. Maas U., Warnatz J. Ignition processes in hydrogen-oxygen mixtures // Combust. Flame. 1988. Vol. 74. P. 53–69.
- [36]. Deuflhard P., Hairer E., Zugck J. One-step and extrapolation methods for differential-algebraic systems // Numer. Math. 1987. Vol. 51. P. 501–516.
- [37]. Deuflhard P., Nowak U. Extrapolation Integrators for Quasilinear Implicit ODEs. Berlin: Springer, 1987. 247 p.
- [38]. Kichatov B., Kolobov A., Gubernov V., Bykov V., Maas U. Combustion of rich hydrogen—air mixture stabilised near a cylindrical porous burner // Combust. Theory Model. 2020. Vol. 24. P. 650—665.
- [39]. Gubernov V., Kolobov A., Bykov V., Maas U. Investigation of rich hydrogen—air deflagrations in models with detailed and reduced kinetic mechanisms // Combust. Flame. 2016. Vol. 168. P. 32—38.
- [40]. Bykov V., Shashidharan S., Berszany E., Gubernov V., Maas U. Model reduction of rich premixed hydrogen/air oscillatory flames by global quasilinearization (GQL) // Combust. Sci. Technol. 2022. Vol. 194. P. 2377–2394.

References

- [1]. V. Gubernov, A. Kolobov, A. Polezhaev, H. Sidhu, G. Mercer, Period doubling and chaotic transient in a model of chain-branching combustion wave propagation, Proc. R. Soc. A Math. Phys. Eng. Sci., 466 (2010) 2747-2769. https://doi.org/10.1098/ rspa.2009.0668
- [2]. V.N. Kurdyumov, V.V. Gubernov, Dynamics of combustion waves in narrow samples of solid energetic material: impact of radiative heat losses on chaotic behavior and dynamical extinction phenomenon, Combust. Flame, 219 (2020) 349-358. https://doi.org/10.1016/j. combustflame.2020.06.014
- [3]. S.B. Margolis, Bifurcation phenomena in burner-stabilized premixed flames, Combust. Sci. Technol., 22 (1980) 143-169. https://doi.org/10.1080/00102208008952379
- [4]. B.J. Matkowsky, D.O. Olagunju, Pulsations in a burner-stabilized premixed plane flame, SIAM J. Appl. Math., 40 (1981) 551-562. https://doi. org/10.1137/0140046

- [5]. J. Buckmaster, Stability of the porous plug burner flame, SIAM J. Appl. Math., 43 (1983) 1335-1349. https://doi.org/10.1137/0143089
- [6]. G. Joulin, Flame oscillations induced by conductive losses to a flat burner, Combust. Flame, 46 (1982) 271-281. https://doi.org/10.1016/0010-2180(82)90021-9
- [7]. A. McIntosh, On the cellular instability of flames near porous-plug burners, J. Fluid Mech., 161 (1985) 43-75. https://doi.org/10.1017/ S0022112085002816
- [8]. H.G. Kaper, G.K. Leaf, B. Matkowsky, On the stability of the porous plug burner flame, Combust. Sci. Technol., 47 (1986) 93-101. https:// doi.org/10.1080/00102208608923867
- [9]. B.H. Chao, C.K. Law, Duality, pulsating instability, and product dissociation in burner-stabilized flames, Combust. Sci. Technol., 62 (1988) 211-237. https://doi.org/10.1080/00102208808924010
- [10]. V.N. Kurdyumov, M. Matalon, The porous-plug burner: flame stabilization, onset of oscillation, and restabilization, Combust. Flame, 153 (2008) 105-118. https://doi.org/10.1016/j. combustflame.2007.07.003
- [11]. B.H. Chao, Instability of burner-stabilized flames with volumetric heat loss, Combust. Flame, 126 (2001) 1476-1488. https://doi.org/10.1016/ S0010-2180(01)00256-5
- [12]. V.N. Kurdyumov, M. Sánchez-Sanz, Influence of radiation losses on the stability of premixed flames on a porous-plug burner, Proc. Combust. Inst., 34 (2013) 989-996. https://doi.org/10.1016/j. proci.2012.06.039
- [13]. S.B. Margolis, Effects of selective diffusion on the stability of burner-stabilized premixed flames, Symp. (Int.) Combust., 18 (1981) 679-693. https:// doi.org/10.1016/S0082-0784(81)80073-2
- [14]. V. Gubernov, V. Bykov, U. Maas, Hydrogen/air burner-stabilized flames at elevated pressures, Combust. Flame, 185 (2017) 44-52. https://doi. org/10.1016/j.combustflame.2017.07.001
- [15]. S. Nechipurenko, T. Miroshnichenko, N. Pestovskii, S. Tskhai, B. Kichatov, V. Gubernov, V. Bykov, U. Maas, Experimental observation of diffusive-thermal oscillations of burner-stabilized methane-air flames, Combust. Flame, 213 (2020) 202-210. https://doi.org/10.1016/j.combustflame.2019.12.016
- [16]. V. Mislavskii, N. Pestovskii, S. Tskhai, B. Kichatov, V. Gubernov, V. Bykov, U. Maas, Diffusive-thermal pulsations of burner-stabilized methane-airflames, Combust. Flame, 234 (2021) 111638. https://doi. org/10.1016/j.combustflame.2021.111638

- [17]. A. Moroshkina, V. Mislavskii, B. Kichatov, V. Gubernov, V. Bykov, U. Maas, Burner-stabilized flames: towards reliable experiments and modelling of transient combustion, Fuel, 332 (2023) 125754. https://doi.org/10.1016/j. fuel.2022.125754
- [18]. A. Moroshkina, E. Yakupov, V. Mislavskii, E. Sereshchenko, A. Polezhaev, S. Minaev, V. Gubernov, V. Bykov, The performance of reaction mechanism in prediction of the characteristics of the diffusive-thermal oscillatory instability of methane-hydrogen-air burner-stabilized flames, Acta Astronaut., 215 (2024) 496-504. https://doi.org/10.1016/j.actaastro.2023.12.032
- [19]. J.W. Mapp, J.I.B. Jr., M. Gorman, Short communication, Combust. Sci. Technol., 43 (1985) 217-225. https://doi. org/10.1080/00102208508947005
- [20]. M. El-Hamdi, M. Gorman, J.W. Mapp, J.I. Blackshear Jr., Stability boundaries of periodic models of propagation in burner-stabilized methane-air flames, Combust. Sci. Technol., 55 (1987) 33-40. https://doi.org/10.1080/00102208708947069
- [21]. H. Pearlman, Target and spiral wave patterns in premixed gas combustion, J. Chem. Soc. Faraday Trans., 93 (1997) 2487-2490. https://doi. org/10.1039/a701506b
- [22]. K. Robbins, M. Gorman, J. Bowers, R. Brockman, Spiral dynamics of pulsating methane-oxygen flames on a circular burner, Chaos, 14 (2004) 467-476. https://doi.org/10.1063/1.1688532
- [23]. C.K. Law, Combustion Physics, Cambridge Univ. Press, 2010.
- [24]. J. Warnatz, U. Maas, R.W. Dibble, Combustion, Springer, 2006.
- [25]. G. Dixon-Lewis, Structure of laminar flames, Symp. (Int.) Combust., 23 (1991) 305-324. https:// doi.org/10.1016/S0082-0784(06)80274-2
- [26]. M. Smooke, Numerical modeling of the structure and properties of tubular strained laminar premixed flames, Dyn. Deflagr. React. Syst., 131 (1991) 125. https://doi.org/10.2514/5.97816008 66043.0125.0144
- [27]. S. Ishizuka, An experimental study on extinction and stability of tubular flames, Combust. Flame, 75 (1989) 367-379. https://doi.org/10.1016/0010-2180(89)90049-7
- [28]. H. Kobayashi, M. Kitano, Extinction characteristics of a stretched cylindrical premixed flame, Combust. Flame, 76 (1989) 285-295. https://doi. org/10.1016/0010-2180(89)90111-9
- [29]. Y. Ogawa, N. Saito, C. Liao, Burner diameter and flammability limit measured by tubular

- flame burner, Symp. (Int.) Combust., 27 (1998) 3221-3227. https://doi.org/10.1016/S0082-0784(98)80186-0
- [30]. Korsakova, V. Gubernov, A. Kolobov, V. Bykov, U. Maas, Stability of rich laminar hydrogenair flames in a model with detailed transport and kinetic mechanisms, Combust. Flame, 163 (2016) 478-486. https://doi.org/10.1016/j. combustflame.2015.10.024
- [31]. V. Bykov, V. Gubernov, U. Maas, Combustion of near stoichiometric hydrogen-air mixtures stabilized near tubular porous burner, Combust. Plasmochem., 20 (2022) 277-278. https://doi. org/10.18321/cpc20(4)277-288
- [32]. G. Stahl, J. Warnatz, Numerical investigation of time-dependent properties and extinction of strained methane and propane-air flamelets, Combust. Flame, 85 (1991) 285-299. https://doi. org/10.1016/0010-2180(91)90134-W
- [33]. V. Giovangigli, Mass conservation and singular multicomponent diffusion algorithms, IMPACT Comput. Sci. Eng., 2 (1990) 73-97. https://doi.org/10.1016/0899-8248(90)90004-T
- [34]. A. Ern, V. Giovangigli, Multicomponent Transport Algorithms, Springer, 1994. https://doi.org/10.1007/978-3-540-48650-3
- [35]. U. Maas, J. Warnatz, Ignition processes in hydrogen-oxygen mixtures, Combust. Flame, 74 (1988) 53-69. https://doi.org/10.1016/0010-2180(88)90086-7
- [36]. P. Deuflhard, E. Hairer, J. Zugck, One-step and extrapolation methods for differential-algebraic systems, Numer. Math., 51 (1987) 501-516. https://doi.org/10.1007/BF01400352
- [37]. P. Deuflhard, U. Nowak, Extrapolation Integrators for Quasilinear Implicit ODEs, Springer, 1987. https://doi.org/10.1007/978-1-4684-6754-3 3
- [38]. B. Kichatov, A. Kolobov, V. Gubernov, V. Bykov, U. Maas, Combustion of rich hydrogen-air mixture stabilised near a cylindrical porous burner, Combust. Theory Model., 24 (2020) 650-665. https://doi.org/10.1080/13647830.2020.1734238
- [39]. V. Gubernov, A. Kolobov, V. Bykov, U. Maas, Investigation of rich hydrogen-air deflagrations in models with detailed and reduced kinetic mechanisms, Combust. Flame, 168 (2016) 32-38. https://doi.org/10.1016/j.combustflame.2016.03.017
- [40]. V. Bykov, S. Shashidharan, E. Berszany, V. Gubernov, U. Maas, Model reduction of rich premixed hydrogen/air oscillatory flames by global quasi-linearization (GQL), Combust. Sci. Technol., 194 (2022) 2377-2394. https://doi.org/10.1080/00102202.2020.1869729

Возникновение термодиффузионной неустойчивости во встречных потоках двойных предварительно перемешанных воздушно-водородных богатых пламен

В. Быков^{1*} и В. Губернов²

¹Технологический институт Карлсруэ, Институт технической термодинамики, Энгельберт-Арнольд-Штрассе 4, корпус 10.91 D-76131 Карлсруэ, Германия ²Физический институт им. П.Н. Лебедева Российской Академии Наук, Ленинский пр., 53, 119991, Москва, Российская Федерация

RNJATOHHA

Эффект возникновения неустойчивости пламени в конфигурации встречного диффузионного двойного пламени исследован численно. Сообщается о возникновении неустойчивости в системе при горании богатого водорода/воздуха и изучаются свойства пульсирующих режимов. Рассматриваются эффекты состава смеси и растяжения, а также давления. Показано что как и в свободно распространяющемся пламени богатой водородвоздушной смеси, возникновение пульсаций стимулируется повышением давления. Увеличение растяжения пламени на противопотоке, как и ожидалось, стабилизирует пламя при высоких значениях растяжений, но, как было обнаружено, способствует возникновению неустойчивости при ее умеренных значениях. Поскольку возникновение колеблющегося пламени чрезвычайно чувствительно к молекулярной диффузии и химической кинетике, результаты исследования можно напрямую проверить в экспериментах. Результаты параметрического исследования вблизи границы и свойства как пульсирующих, так и стационарных режимов можно использовать как источник для дополнительной проверки моделей горения.

Ключевые слова: противоточное пламя водорода, термодиффузионная неустойчивость, возникновение пульсаций, валидация модели.

Бұрын қарсы ток режимінде араласқан сутегі мен ауамен байытылған қос жалында термодиффузиялық тұрақсыздықтың пайда болуы

В. Быков1* және В. Губернов2

¹Карлсруэ технологиялық институты, Техникалық термодинамика институты, Энгельберт-Арнольд-Штрассе 4, корпус 10.91 D-76131 Карлсруэ, Германия ²Физикалық институты Ресей Ғылым Академиясының П.Н. Лебедева, Ленин даңғылы, 53, 119991, Мәскеу, Ресей Федерациясы

АҢДАТПА

Қарсы диффузиялық қос жалын конфигурациясында басталған жалын тұрақсыздықтарының әсері сандық түрде зерттеледі. Бай сутегі/ ауа жану жүйесінде тұрақсыздықтың пайда болуы туралы хабарланады және пульсирленген ерітінділердің қасиеттері зерттеледі. Қоспаның құрамы мен деформация жылдамдығының, сондай-ақ қысымның әсері қарастырылады. Еркін таралатын бай сутегі/ауа жалындары сияқты пульсацияның басталуы қысымның жоғарылауына ықпал етеді. Күтілетіндей жоғарылаған деформация жылдамдығы штаммның жоғары мәндері үшін жалынды тұрақтандырады, бірақ қалыпты мәндер үшін тұрақсыздықтың басталуына ықпал ететіні анықталды. Тербелмелі жалын әрекетінің басталуы молекулалық диффузияға және химиялық кинетикаға өте сезімтал болғандықтан, зерттеу нәтижесін эксперименттерде тікелей тексеруге болады. Шекара маңындағы параметрлік зерттеу нәтижелерін және пульсирленген және тұрақты ерітінділердің қасиеттерін қосымша жану үлгілерін тексеру үшін пайдалануға болады.

Түйінді сөздер: сутектің қарама-қарсы жалыны, термодиффузиялық тұрақсыздық, толқындардың пайда болуы, модельдің валидациясы.

Сведения об авторах

В.В. Быков — научный сотрудник, доцент, Технологический институт Карлсруэ, Институт технической термодинамики, Германия E-mail: viatcheslav.bykov@kit.edu

ORCID 0000-0002-2274-8410

В.В. Губернов — главный научный сотрудник, зав. лабораторией динамики реагирующих систем, Физический институт им. П.Н. Лебедева Российской Академии Наук, Российская Федерация E-mail: v.v.gubernov@xmail.ru
ORCID 0000-0001-5821-8641